Multi-targeting aurones with monoamine oxidase and amyloid-beta inhibitory activities: structure-activity relationship and translating multi-potency to neuroprotection

It is advisable to refer to the publisher's version if you intend to cite from the work. See Guidance on citing.

To link to this article DOI: http://dx.doi.org/10.1016/j.biopha.2018.11.054

Publisher: Elsevier

www.reading.ac.uk/centaur

CentAUR

Central Archive at the University of Reading

Reading's research outputs online

Multi-targeting aurones with monoamine oxidase and amyloid-beta inhibitory activities: Structure-activity relationship and translating multi-potency to neuroprotection

Kok-Fui Liew[b], Elaine Hui-Chien Lee[a], Kit-Lam Chan[a], Chong-Yew Lee[a],[*]

[a] School of Pharmaceutical Sciences, Universiti Sains Malaysia, 11800 Penang, Malaysia
[b] School of Pharmacy, University of Reading Malaysia, 79200 Johor, Malaysia

ARTICLE INFO

ABSTRACT

Previously, a series of aurones bearing amine and carbamate functionalities was synthesized and evaluated for their cholinesterase inhibitory activity and drug-like attributes. In the present study, these aurones were evaluated for their multi-targeting properties in two Alzheimer's disease (AD)-related activities namely, monoamine oxidase (MAO) and amyloid-beta (Aβ) inhibition. Evaluation of the aurones for MAO inhibitory activity disclosed several potent selective inhibitors of MAO-B, particularly those with 6-methoxyl group attached at ring A. Of the different amine moieties attached as side chains, pyrrolidine-bearing aurones were prominent as represented by 2-2, the most potent inhibitor. Evaluation on the Aβ aggregation inhibition identified 4-3 as the best inhibitor with a percentage inhibition comparable to that of a known Aβ inhibitor curcumin. Examination on the neuroprotective ability of the more drug-like aurone 4-3 in two Caenorhabditis elegans neurodegeneration models showed 4-3 to protect the nematodes against both Aβ- and 6-hydroxydopamine-induced toxicities. These new activities further support 4-3 as a promising lead to develop the aurones as potential multipotent agents for neurodegenerative diseases.

1. Introduction

Alzheimer's disease (AD) is one of the most common causes of mental decline in the aging population. Notwithstanding efforts to understand the AD pathogenesis, the precise etiology of AD remains incomplete [1]. Histopathological hallmarks including low levels of acetylcholine (ACh), amyloid-beta (Aβ) accumulation, tau protein aggregation, and oxidative stress have been associated with the AD pathogenesis, and several hypotheses based on these factors were proposed to explain the cause of AD progression [2–5].

The cholinergic hypothesis is particularly important as it has been the cornerstone to the discovery of the present treatments for AD [2,6]. This hypothesis postulates that the cognitive impairment and symptoms (dementia, memory loss) experienced by AD patients is due to the extensive loss of cholinergic neurons in certain regions of the brain such as the hypothalamus, amygdala, and neocortex. Drugs such as acetylcholinesterase (AChE) inhibitors that can restore this cholinergic deficit in the central nervous system (CNS) would therefore be able to slow the cognitive decline associated with AD. Also of prominence is the amyloid cascade hypothesis, which originates from the observation

of Aβ plaques in the AD brains [3]. The deposition of insoluble Aβ fibrils amidst the neurons and the aggregation of Aβ monomers into protofibrils and oligomers were shown in studies in vitro and in vivo to be toxic to the neurons [7]. Accordingly, agents that target Aβ and inhibit its aggregation are being sought after [8]. In addition, evidence points to the role of alterations in the monoaminergic neurotransmitter system and the resulting oxidative stress in AD [9–11]. In a recent study, gamma-aminobutyric acid (GABA) secretion by reactive astrocytes linked to MAO-B activity was found to lead to memory impairment in mice and that inhibiting MAO-B restored the learning, memory, and synaptic plasticity of the mice [12]. The development of MAO-B inhibitors ladostigil [13] and RO4602522 [14] as potential therapeutics for AD also lends support for MAO inhibition as a potential approach in treating AD.

Due to the multifactorial nature of AD, attention has shifted to a multi-targeting approach, the idea of a multi-target directed ligand (MDTL) that engages several biological target proteins simultaneously [15–17]. In an earlier report [18], we have synthesized a series of anticholinesterase aurone derivatives that carry various basic amines (dimethylamino-, piperidine, and pyrrolidine alkyls) and

* Corresponding author.
  E-mail address: chongyew@usm.my (C.-Y. Lee).

Table 1
Structures of compounds in Series. 1 to 6.
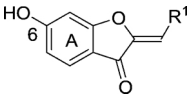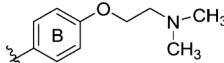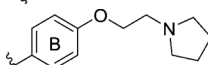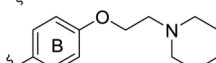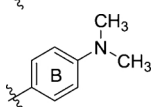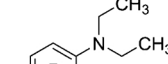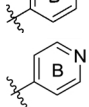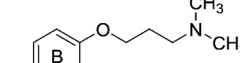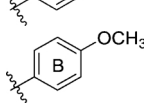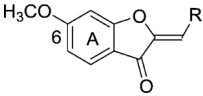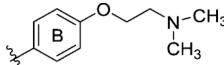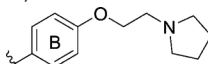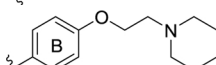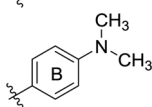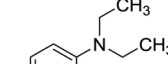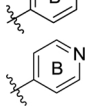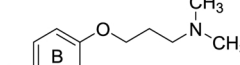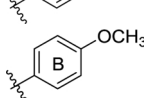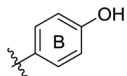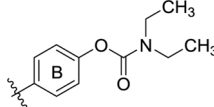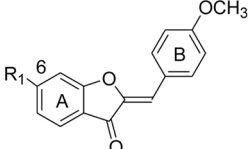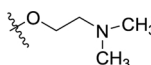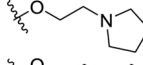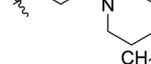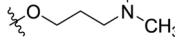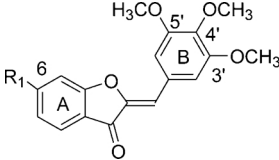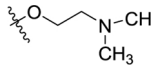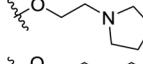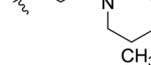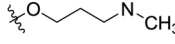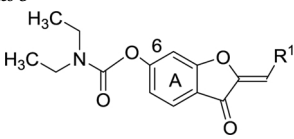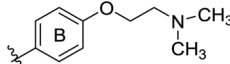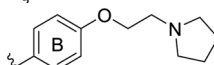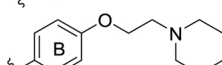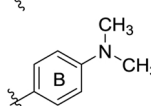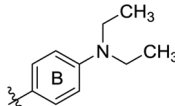
Compound	R¹

Series 1

1-1	
1-2	
1-3	
1-4	
1-5	
1-6	
1-7	
1-8	

Series 2

2-1	
2-2	
2-3	
2-4	
2-5	
2-6	
2-7	
2-8	

Table 1 (*continued*)

Compound	R¹
2-9	
2-11	

Series 3

3-1	
3-2	
3-3	
3-7	

Series 4

4-1	
4-2	
4-3	
4-7	

Series 5

5-1	
5-2	
5-3	
5-4	
5-5	

Table 1 (*continued*)

Compound	R¹
5-6	B ring, O(CH₂)₃N(CH₃)₂
5-7	B ring, OCH₃
Series 6	H₃CO– A/benzofuranone scaffold (position 6) =CH–R¹
6-1	B ring, 3'-Cl, O(CH₂)₂N(CH₃)₂
6-2	B ring, 3'-Cl, O(CH₂)₂-pyrrolidine
6-3	B ring, 3'-Cl, O(CH₂)₂-piperidine
6-7	B ring, 3'-Cl, O(CH₂)₃N(CH₃)₂
6-8	B ring, 2'-Cl, O(CH₂)₂N(CH₃)₂
6-9	B ring, 2'-Cl, O(CH₂)₂-pyrrolidine
6-10	B ring, 2'-Cl, O(CH₂)₂-piperidine
6-11	B ring, 2'-Cl, O(CH₂)₃N(CH₃)₂

diethylcarbamate at rings A and B of the scaffold (Table 1). Several promising AChE-inhibiting aurones (submicromolar IC_{50}s) that bear amine functionalities were uncovered. The aurones also exhibited high passive permeability in the parallel artificial membrane permeability assay for blood-brain barrier (PAMPA-BBB) ($P_e > 20 \times 10^{-6}$ cm/s), a feature favourable for CNS-active drugs. Aurone **4-3** was identified as the optimal cholinesterase inhibitor (AChE IC_{50} 0.43 μM; BuChE IC_{50} 6.15 μM) with high BBB permeability in both PAMPA-BBB and a brain endothelial cell model [19] as well as satisfactory metabolic stability ($T_{1/2}$ in rat liver microsomes = 44.3 min). In our development of an MDTL for AD, we chose to re-examine these aurones without further modification of their structures in keeping their sizes small (molecular weights < 500 Da) and within drug-like limits.

To repurpose the aurones as multi-targeting agents, herein we report the evaluation of these compounds in two AD-related activities *in vitro*: monoamine oxidase (MAO) inhibition and self-induced amyloid-beta (Aβ) aggregation inhibition. The rationale of targeting these two proteins was prompted by reports of aurones with simpler structures exhibiting modest MAO inhibition [20,21] and their high binding affinity for Aβ aggregates *in vitro* as Aβ probes [22]. Subsequently, the most promising aurone with a good combination of multi-targeting and

drug-like properties was selected for evaluation in two *Caenorhabditis elegans* neurodegeneration models namely, Aβ-induced paralysis and 6-hydroxydopamine (OHDA)-induced neurodegeneration to determine whether these desirable attributes could be translated to efficacious neuroprotection in a whole organism.

2. Materials and methods

2.1. Evaluation of inhibitory effect on monoamine oxidase enzymes

Recombinant human MAO-A and MAO-B enzymes were purchased from BD Biosciences (San Jose, CA). Tyramine, benzylamine, clorgyline hydrochloride, vanillic acid, 4-aminoantipyrine and horseradish peroxidase were obtained from Sigma-Aldrich (St Louis, MO). Donepezil hydrochloride and pargyline hydrochloride were purchased from Santa-Cruz Biotechnology Inc. (CA, USA). Sodium dihydrogen phosphate anhydrous was purchased from R&M chemicals (Essex, UK), disodium hydrogen phosphate anhydrous from Merck (Darmstadt, Germany), 96-well microplates from Greiner Bio-one (Frickenhausen, Germany). All other materials were purchased from Sigma-Aldrich (Dorset, UK) unless otherwise stated. Stock solutions of test compounds were prepared using dimethyl sulfoxide (DMSO) at a concentration of 2 mg/ml. These were diluted with the reaction medium to the final concentrations during the assay. All compounds are initially tested at a concentration of 50 μM and aurones that displayed percentage inhibition of more than 75% at the stated concentration were further selected to determine their IC_{50} based on the corresponding enzyme.

The MAO inhibition activities were evaluated using a coupled colorimetric method as described previously [23]. 0.2 M potassium phosphate buffer (pH 7.6, 140 μL) was pre-incubated with sample solution (20 μL), and MAO-A or MAO-B enzyme (20 μL) at 37 °C for 15 min. The final concentration of the MAO-A and MAO-B enzymes in the final reaction mixture were 0.1 mg/mL and 0.2 mg/mL respectively. Following the incubations, the enzymatic reactions were initiated by adding 10 μL of 15 mM tyramine (for MAO-A) or benzylamine (for MAO-B); followed by 10 μl of a chromogenic solution containing vanillic acid (4 mM), 4-aminoantipyrine (2 mM), and horseradish peroxidase (60 U/mL). The rate of absorbance change, reflecting the MAO activity was measured at 490 nm for 30 min at 37 °C with a Multiskan FC Microplate Photometer (Thermo Fisher Scientific, MA, US). Each assay was carried out with clorgyline or pargyline as positive controls. The percentage inhibition was calculated using the following equation:

$$\% \ inhibition = (A_{treated} - A_{blank})/(A_{untreated} - A_{blank}) \times 100$$

where $A_{treated}$ is the absorbance of the compound-treated well, $A_{untreated}$ is the well without compound, and A_{blank} is a well filled only with phosphate buffer. Compounds with percent inhibition greater than 75% were further tested at different concentrations to determine IC_{50} values obtained from the inhibition *versus* concentration curves plotted using GraphPad Prism 4.0 (La Jolla, CA, USA). The reactions were performed in three independent runs and each run of a sample was performed in triplicates.

2.2. Evaluation of inhibitory effect on self-induced Aβ₁₋₄₀ aggregation

Human amyloid-beta (Aβ₁₋₄₀) peptide, thioflavin T (ThT), hexafluoroisopropanol (HFIP), DMSO and curcumin were obtained from Sigma-Aldrich (St Louis, MO). Prior to the assay, the lyophilized Aβ₁₋₄₀ was reconstituted in HFIP at a concentration of 1 mg/mL followed by freeze-drying under vacuum to obtain Aβ₁₋₄₀ monomers. The monomers were stored at 4 °C and used fresh for the assay. Test compounds were dissolved in DMSO and diluted to the final assay concentration (25 μM) with the assay medium. Thioflavin T-based fluorometric assay was performed based on a reported method [28] with slight modifications to investigate the self-induced Aβ₁₋₄₀ aggregation inhibition of selected

aurones. In brief, the pre-treated Aβ_{1-40} monomer (25 μM, final concentration) was incubated with the test compounds (25 μM, final concentration) and ThT (10 μM) in 0.05 M phosphate buffer (pH 7.4) at 37 °C for 48 h. The ThT fluorescence intensity was measured using LS-45 luminescence spectrometers (Perkin Elmer, Inc., Waltham, MA, USA) with excitation and emission wavelengths of 440 nm 484 nm respectively over a time period of 48 h. The assay was performed in three independent runs. Each run of a sample was performed in triplicates and the percentage inhibition was calculated by using the following formula:

% Inhibition $= (1 - Fi/Fc) \times 100$

in which Fi and Fc are the fluorescence intensities obtained from Aβ aggregation in the presence and absence of inhibitors respectively after subtracting the background reading.

2.3. Synthesis of the hydrochloride salt of aurone 4-3 (4-3 HCl)

The reagents for synthesis (synthetic grade or better) were obtained from Sigma-Aldrich Chemical Company Inc. (Singapore) and Acros Organics (Geel, Belgium) and used without further purification. A scale-up synthesis of 4-3 was performed according to the procedure described in the previous work [18]. Subsequently, to a solution of 4-3 in diethyl ether (500 mg, 1.139 mmol, 100 mL/mmol) was added dropwise concentrated hydrochloric acid (2 mL). The reaction mixture was then left stirring at room temperature until the appearance of yellow precipitates (1 h). The precipitated hydrochloride salt was filtered, washed three times with diethyl ether and dried to yield the hydrochloride salt form of 4-3 (4-3 HCl) as a yellow solid, 82.16% yield; m.p. 228–230 °C; ^{1}H NMR (DMSO-d_6, 500 MHz): δ 7.74 (d, J = 8.6 Hz, H4), 7.35, (s, 2 H), 7.29 (d, J = 1.8 Hz, H7), 6.92 (dd, J = 8.6, 1.8 Hz, H5), 6.84 (s, 1 H), 4.61 (t, J = 4.9 Hz, 2 H), 3.87 (s, 6 H), 3.74 (s, 3 H), 3.49–3.53 (m, 4 H), 2.97–3.04 (m, 2 H), 1.79–1.82 (m, 4 H), 1.68–1.72 (m, 1 H), 1.34–1.43 (m, 1 H); ^{13}C NMR (DMSO-d_6, 125 MHz): δ 182.1 (CO), 168.1, 165.8, 153.5, 147.1, 139.8, 127.8, 126.0, 114.9, 113.6, 112.2, 109.5, 98.7, 63.8, 60.7, 56.5, 54.8, 53.1, 22.8, 21.6; HRMS (TOF-ES) calcd for C$_{25}$H$_{30}$NO$_6^+$ ([M + H]$^+$): 440.2073, found 440.2073; HPLC analyses: t_R = 2.67 min (99.83% pure at 260 nm; 99.79% pure at 330 nm) on the C18 analytical column; Mobile phase: solvent system A (MeOH 55% and 0.1% HCOOH in H$_2$O); t_R = 4.78 min (97.56% pure at 260 nm; 98.13% pure at 330 nm) on the C18 analytical column; Mobile phase: solvent system B (CH$_3$CN 30% and 0.1% HCOOH in H$_2$O).

2.4. Caenorhabditis elegans (C. elegans) neuroprotection assay

2.4.1. Materials
Microbiology agar, sodium chloride and peptone were obtained from Merck (Darmstadt, Germany). Calcium chloride, disodium hydrogen phosphate, dipotassium hydrogen phosphate, magnesium sulphate and potassium dihydrogen phosphate were purchased from R&M Chemicals (Essex, UK). 6-hydroxydopamine (6-OHDA), dimethyl sulfoxide (DMSO), Luria Bertani (LB) broth and cholesterol were all purchased from Sigma-Aldrich (St. Louis, USA), Luria Bertani (LB) agar from Miller (Mumbai, India), and penicillin-streptomycin solution (10,000 units/mL) from Hyclone (Thermo Scientific, Utah, USA). The petri dishes (60 mm and 35 mm diameter) were obtained from Corning (Corning Inc., New York, USA) and centrifuge tubes (15 mL and 50 mL) were from Techno Plastic Products (Trasadingen, Switzerland). The 1-inch piece of 32 gauge platinum wire was product of Bio-Rad Laboratory (Hercules, USA).

2.4.2. C. elegans strains and maintenance
The Aβ-expressing transgenic strain GMC101 (dvIs100 [unc-54p::A-beta-1-42::unc-54 3′-UTR + mtl-2p::GFP]. mtl-2p::GFP) and the GFP-labelled DAergic neuron strain UA57 (baIs4 [dat-1p::GFP + dat-

1p::CAT-2]; GFP expression in CEP, ADE and PDE neurons) as well as their food source *Escherichia coli* (*E.coli*) strain OP50 were obtained from the *Caenorhabditis* Genetics Center (University of Minnesota, MN, US). For normal maintenance purposes, the *C. elegans* strains were routinely propagated at 16 °C on solid nematode growth medium (NGM) agar in petri plates, which was pre-seeded with spots of *E.coli* OP50 as food source.

2.4.3. Preparation of nematode growth medium (NGM) agar
17.0 g of microbiology grade agar, 2.5 g of peptone and 3.0 g of sodium chloride were accurately weighed into an autoclavable bottle and dissolved in 975 mL of distilled water. The mixture was autoclaved at 121 °C for 20 min. The agar was then allowed to cool down to 55 °C in the autoclave. Subsequently, 1 mL of 1 M calcium chloride, 1 mL of 5.0 mg/ml cholesterol in ethanol, 1 mL of 1 M magnesium sulphate and 25 ml of 1 M potassium phosphate buffer were aseptically added to the agar mixture. The NGM agar was then poured into sterile petri plates and allowed to dry in laminar flow hood (Isocide™, Esco, Singapore). For the normal maintenance purposes, 60 mm diameter of agar plate was used (11 ml of agar) while 35 mm diameter agar plate (5.0 ml of agar) was used as the test plates. After drying, the agar plates were left at room temperature for 2 days in an air-tight container before seeding with the OP50 solution.

2.4.4. Preparation of food source (OP50)
2.5 g of LB broth powder was weighed into an autoclavable bottle and dissolved in 100 mL of distilled water. The mixture was autoclaved (Hirayama, Japan) for 20 min at 121 °C. The autoclaved LB broth was then allowed to cool to room temperature and 1 mL of penicillin-streptomycin solution was added. Subsequently, a single colony of OP50 from a streak plate was inoculated in the sterile LB broth and left to incubate on a shaker (Grant-Bio, England) for 2 days at room temperature. After the incubation, the OP50 solution was equally separated into four 50 mL-centrifuge tube with each of the tubes containing 25 mL of the OP50 solution. The OP50 solutions were then centrifuged at 2000 × g for 40 min at 4 °C and the pellets of OP50 were collected after the supernatant was discarded. The OP50 pellets were later resuspended in 5 mL of fresh LB broth and seeded onto the NGM plates (600 μl was seeded onto the 60 mm diameter plates and 100 μL for the 35 mm diameter test plates) as food source.

2.4.5. Preparation of test plates
Stock solution of 4-3 HCl was prepared using distilled water at a concentration of 10 mM. The stock solution was then added directly to the molten NGM agar at 55 °C during the NGM agar preparation and mixed well to obtain final concentrations of 25, 50 and 100 μM in the NGM agar test plates. Since distilled water was used as the carrier to dissolve the compound, a carrier control plate was not required for the assay. Control plates (without test compound) prepared consisted only of the NGM agar.

2.4.6. Aβ-induced paralysis assay
The Aβ-expressing transgenic *C. elegans* GMC101 maintained on NGM plates (60 mm diameter petri plates) at 16 °C were used in the paralysis assay. The test plates were prepared as described in the Section 2.4.5. The paralysis assays were performed according to the method described by Dostal and Link [24]. In brief, egg-synchronised population of the transgenic worms was prepared by allowing gravid adult worms to lay eggs onto the NGM test plate (with or without test compound) spread with OP50 for 2 h at 16 °C. The gravid adults were then removed and plates containing the eggs were incubated at 16 °C. At 68 h post egg-lay, the transgene expression was induced by up-shifting the temperature from 16 to 25 °C and maintained until the end of the paralysis assay. Paralysis was scored starting at 24 h after induction and the scoring was performed at 2 h intervals. Worms were scored as paralysed if they failed to respond to a touch-provoked

movement with a platinum wire. The assays were performed in three independent runs and each run of a sample was performed in triplicates with approximately 55–75 worms per test plates.

2.4.7. 6-hydroxydopamine (6-OHDA)-induced dopaminergic neurodegeneration assay

The neuroprotective effects of **4-3 HCl** against 6-OHDA-induced dopaminergic neuronal cell death was evaluated following the protocol described by Maranova and Nichols [25]. The transgenic *C. elegans* UA57 nematodes, with GFP expression in their dopaminergic neurons maintained on NGM plates (60 mm diameter petri plates) at 16 °C were used in the assay. The test plates were prepared as described in the Section 2.4.5. The egg-synchronised population of the transgenic worms was prepared by allowing gravid adult worms to lay eggs onto the NGM test plate (in the presence or absence of compound) spread with OP50 for 2 h at 16 °C. The gravid adults were then removed and plates containing the eggs were incubated for 19 h at 16 °C till they reach the L1 stage. The synchronous L1 worms were then washed twice with M9 buffer and resuspended in the buffer. The 6-OHDA-induced dopaminergic neurodegeneration was initiated by exposing the synchronous populations of L1 worms to 6-OHDA solution (5 mM 6-OHDA in 1% DMSO) and incubated at room temperature under dark conditions for 1 h with gentle agitation every 10 min. After the incubation, the worms were washed 3 times with M9 buffer and subsequently incubated in NGM test plates (in the presence or absence of compound) pre-seeded with OP50 at 20 °C for 72 h before the evaluation of neuronal death. After 72 h of incubation, the worms were washed 3 times with M9 buffer and then mounted onto a 2% agar pad on glass slide enclosed with a cover slip. Imaging of the worms was carried out with an inverted fluorescence microscope (Carl Zeiss MicroImaging GmbH, Göttingen, Germany). Fluorescent images of the head region of the worms were taken using AxioVision software (Carl Zeiss, Göttingen, Germany). The dopaminergic neuronal death of the worms was determined by the diminished, reduced, or absence of the dopaminergic neuron GFP fluorescence. The assays were performed in three independent runs and each run of a sample was performed in triplicates with at least 35 worms per test plates analyzed.

2.4.8. Statistical analysis

Statistical analyses were performed using GraphPad Prism 5.0 software (La Jolla, CA, USA). The data were analyzed using one-way ANOVA when comparing the differences between groups, except for the comparison of survival curve data in the paralysis assay, which was performed using the log-rank (Mantel-Cox) test of the Kaplan-Meier survival function. Data were presented as mean ± SEM. The differences were considered statistically significant when *p* values were < 0.05.

3. Results and discussion

3.1. The MAO inhibitory activity of the aurones

The synthesis of the aurones (Series 1 to 6) was reported previously [18]. The aurones were initially screened at 50 μM for the inhibition against two human MAOs, *h*MAO-A and *h*MAO-B. Clorgyline (a selective MAO-A inhibitor) and pargyline (a selective MAO-B inhibitor) were used as positive controls for the *in vitro* assay and the obtained inhibitory concentrations were compared with the IC$_{50}$ values from the literature [26,27]. Donepezil, a known AChE inhibitor was also included in the evaluation to determine the multi-potency of the compound and compare it with that of the aurones, some of which were previously identified as AChE inhibitors [18]. A threshold value of 75% inhibition was arbitrarily set for selecting compounds for further determination of their IC$_{50}$ (Fig. 1).

As shown in Fig. 1, most aurones exhibited selectivity towards MAO-B inhibition over MAO-A inhibition in varying degrees. As all

aurones across the six series showed low MAO-A inhibition (< 75%), they were deemed weak MAO-A inhibitors and their activities for this MAO subtype was not pursued further. Irrespective of the substituents at ring B of the scaffold, an outstanding MAO-B inhibitory activity was observed in Series 2 (6-methoxyaurones), with 8 out of 10 compounds inhibiting MAO-B by more than 75% (Fig. 1). Clearly, the placement of a 6-methoxyl group at ring A of the compounds provided favourable MAO-B inhibitory activity. However, a substitution of the bulkier carbamoyl group at the same position (6-carbamoyl) of ring A as seen in Series 5 resulted in lower inhibition against MAO-B. None of the 6-carbamoylaurones in this series showed inhibition at 75% and above (Fig. 1) and they were excluded from further evaluation. Changing the position of the methoxyl group at ring A (**2-2**) to ring B led to a slightly lower activity as seen in Series 3 aurones (**3-2**). In addition, placing three methoxyl groups at ring B as seen in Series 4 aurones (**4-2**) did not affect significantly their activities when compared to Series 3 aurones with the same amine (pyrrolidine) moiety. Another notable observation was between Series 2 and Series 6. The main scaffold in Series 6 aurones was structurally related to Series 2 aurones except for the presence of an additional 2′-chloro (**6-8**, **6-9**, **6-10**, **6-11**) and 3′-chloro (**6-1**, **6-2**, **6-3**, **6-7**) at ring B. The presence of 2′-chloro (**6-9**) and 3′-chloro (**6-2**) atom on the better MAO inhibitors among the 6-methoxyaurones (percentage inhibition > 75%, for example **2-2**) resulted in a decline in MAO-B inhibition. To refine the structure-activity relationship for better comparison between the compounds, the aurones that exhibited more than 75% inhibition against MAO-B were selected for the determination of their IC$_{50}$ values over a range of concentrations (Table 2).

A different SAR was observed for MAO-B inhibition when compared to their AChE inhibitory activity as determined previously [18]. It is interesting to find that aurones bearing the pyrrolidine moiety exhibited prominent MAO-B inhibition across the six series (Table 2). Aurones bearing piperidine (which were good AChEIs in the earlier report) had low inhibition or were devoid of activities (IC$_{50}$s > 50 μM). The most active aurone identified was **2-2** (4′-O-ethyl pyrrolidine at ring B) with a submicromolar IC$_{50}$ of 0.895 μM. Non-cyclic amine bearing aurones (dimethylaminoethyl and dimethylaminopropyl) and those with weakly basic nitrogen moieties (pyridinyl and aniline) showed low to moderate inhibition (2.35–8.18 μM) against MAO-B. On the other hand, derivatives without any amine or nitrogen functionalities (**1-8**, **2-8**) showed moderate MAO-B inhibition indicating an inherent feature of the aurone scaffold itself as an MAO inhibitor. The presence of amine moieties (of any types) in the aurone scaffold is necessary for its cholinesterase inhibition but for the inhibition of MAO-B, the pyrrolidine amine is particularly important.

In two recent reports on aurones showing MAO inhibitory activity [20,21], several aurones were identified as MAO inhibitors with moderate potencies. The reported aurones shared similarities with a few compounds of the present study such as the ring B 4′-aminoaurones (**1-4**, **1-5**, **2-4**, **2-5**) and 6,4′-dimethoxyaurone (**2–8**) which also showed moderate potencies. The simplicity of their structures and the lack of elaborate functionalization again underscored the intrinsic property of the scaffold to bind to MAO. However, the prominence of the pyrrolidine moiety (for example, **2-2**) and the 6-methoxyl group (Series 2) in most of the active aurones uncovered presently indicated that improvement in MAO inhibition activity may still be rendered with further elaboration of the scaffold.

3.2. Aβ$_{1-40}$ aggregation inhibitory effect of the aurones

Next, the Aβ anti-aggregation property of selected aurones was evaluated using the Thioflavin T (ThT) spectrofluorometric assay. ThT is a benzothiazole salt used as a dye to quantify the fibrillisation of misfolded protein aggregates, both *in vitro* and *in vivo*. The principle of this assay is based on the measurement of fluorescence intensity change of ThT upon binding to the Aβ fibrils. Aβ monomers in DMSO were dissolved in an aqueous buffer and allowed to aggregate and form
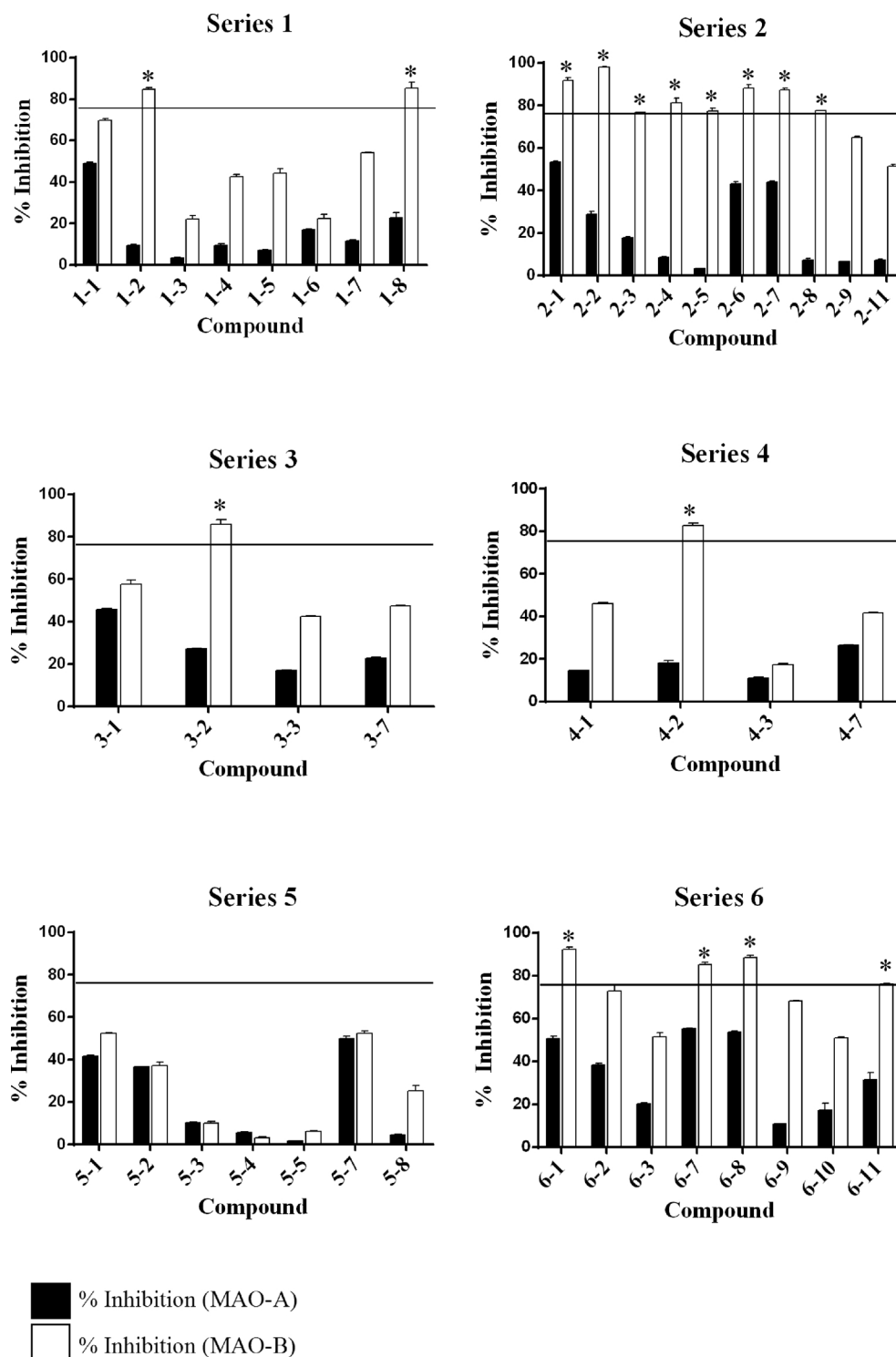
Fig. 1. MAO-A and MAO-B inhibitory activities expressed in percentage inhibition (n = 3) for Series 1-6 aurones at 50 μM. (*) indicates compounds with % inhibition = / > 75%.

amyloid fibrils. As Aβ fibrils were formed, the ThT added would bind to the fibrils and the fluorescence intensity was measured over a 48 h period.

Several aurones were selected for this evaluation on the basis of their promising AChE [18] and MAO-B inhibitory activities. They were **2-2**, **2-3**, **3-3**, **4-3** and **6-3**. The aurone without any amine moieties (**2-8**) was also included to examine the Aβ anti-aggregation properties of the simple, unfunctionalized aurone scaffold. Curcumin, a known inhibitor of Aβ aggregation was used as a positive control for the assay by

comparing the percentage inhibition at 25 μM with the reported value [28]. Donepezil, an AChEI was also included in the assay to assess whether it has Aβ anti-aggregation property considering the structural similarity of the drug with the aurones.

The changes in ThT fluorescence intensity (reflecting the Aβ fibrillisation process) of incubations of Aβ with the test compounds or without compound (negative control) over 48 h were monitored (Fig. 2). It was found that after 8 h, the aggregation of Aβ (negative control) incubated at 37 °C in sodium phosphate buffer (pH 7.4)

Table 2
MAO-B inhibitory activities (IC_{50}) of selected aurones.

Compound	IC_{50} MAO-B	
	Mean (µM)[a]	SEM (µM)[a]
Donepezil	63.8	1.28
Clorgyline	18.7	0.34
Pargyline	0.92	0.16
Series 1		
6-Hydroxyaurones		
1-2	5.06	1.06
1-8	1.42	0.28
Series 2		
6-Methoxyaurones		
2-1	2.35	1.06
2-2	0.895	0.18
2-3	13.3	1.10
2-4	7.56	1.23
2-5	5.04	1.09
2-6	3.41	1.08
2-7	5.41	1.08
2-8	8.18	1.09
Series 3		
4'-Methoxyaurones		
3-2	2.38	1.07
Series 4		
3',4',5'-Trimethoxyaurones		
4-2	4.05	1.07
Series 6		
3'-Chloroaurones		
6-1	1.57	0.54
6-7	1.57	0.52
2'-Chloroaurones		
6-8	1.37	0.21
6-11	1.42	0.23

[a] determined in three independent experiments (n = 3).

Table 3
Aβ anti-aggregation activity of test compounds (25 µM) at 24 h timepoint.

Compound	Mean (% inhibition)	SD[b]
Curcumin	30.51[a]	3.83
Donepezil	7.56[a]	10.11
2-8	20.92[a]	2.11
2-2	0.46[a]	4.19
2-3	5.90[a]	4.57
3-3	7.83[a]	2.15
4-3	36.13[a]	9.99
6-3	23.78[a]	0.55

[a] Determined at 24 h.
[b] Standard deviation (n = 3).

slightly better Aβ inhibitor (5.9%) compared to 6-methoxyaurone **2-2** (0.46%) bearing a pyrrolidine moiety which was considered inactive. Switching the position of the methoxyl group from ring B to ring A as seen in **2-3** *versus* **3-3** did not affect the inhibition activity. Interestingly, aurone **4-3** with three methoxyl groups placed at ring B was identified as the best Aβ aggregation inhibitor where it exhibited the highest percentage of Aβ aggregation inhibition (36.13%) at 25 µM, slightly better than curcumin. The placement of the three methoxyl groups (*versus* on a single methoxyl as in **3-3**) at ring B of the aurone framework appeared favourable in inhibiting Aβ. On the other hand, the aurone without any amine moieties (**2-8**) also showed a better inhibition (20.9%) against Aβ aggregation compared to the AChEI donepezil (7.56%), indicating the inherent property of the scaffold itself to bind to the Aβ monomer and inhibit Aβ fibrillisation.

From these two assays, a multi-targeting potential is uncovered in two aurones with anticholinesterase activity: **2-2** with good MAO-B inhibition activity, and **4-3** which can inhibit Aβ. However, examining the previously reported drug-like profiles of compounds **2-2** and **4-3**, **4-3** was considered the better drug-like lead. **4-3** possessed the best CYP450 metabolic stability in the *in vitro* rat liver microsomal incubation ($T_{1/2}$ 44 min, *versus* **2-2** with $T_{1/2}$ 5 min) and was highly BBB permeable in both the PAMPA assay and a brain endothelial cell model [19]. Therefore, it was singled out to determine whether its the multi-targeting and drug-like attributes could lead to efficacious neuroprotection in the two *C. elegans* neurodegeneration models: Aβ-induced paralysis and 6-OHDA-induced neurodegeneration. One of the limitations of these *C. elegans* assays is the need to use significant amounts of organic solvents and solubilisers such as DMSO, ethanol, methanol, or Tween 20 to solubilise a test compound which may affect the assay outcome as these solvents/solubilisers are known to cause toxicity and may affect the general health of the *C. elegans* [29,30]. Moreover, given the amount of the test compound to be incorporated into the assay medium (5 mL of agar), there is a certain limitation to the solubility of **4-3** in the aqueous medium used in the assays. Therefore, to avoid these circumstances, a readily water-soluble hydrochloride salt of **4-3** (**4-3 HCl**) was synthesized and used for the evaluation of neuroprotection in the *C. elegans* models.

reached a plateau which remained until the end of the monitoring period. The fluorescence intensities for curcumin, **4-3**, **6-3** and **2-8** was observed to maintain at the range of 0.2 to 0.25 units after they reached plateau at 8 h onwards, indicating that these compounds inhibited the Aβ aggregation to certain extents. On the other hand, aurone **2-2**, **2-3** and **3-3** were inactive in inhibiting Aβ aggregation as their fluorescence intensity curves showed similar profiles to that of the negative control. For better comparison of the extent of anti-aggregation displayed by the compounds, the percentages of inhibition on Aβ aggregation at the 24 h timepoint were determined (Table 3).

The Aβ anti-aggregation activity of the aurones ranged from 0.46 to 36.1% at 24 h (Table 3). Curcumin, a known Aβ aggregation inhibitor [28] was found to inhibit Aβ aggregation by 30.5% at 25 µM. By examining the structures of the selected aurones and their inhibitory activities, an important structure-activity relationship could be made. The 6-methoxyaurone **2-3** bearing a piperidine moiety was observed to be a

Fig. 2. Aβ aggregation curves for test compounds (25 µM) over 48 h.

A

Treatment of **4-3 HCl**

68 hours incubation at 16 °C   24 hours

Egg

0   L1   L2   L3   L4   Paralysis scoring   End of paralysis

Scoring at 2 hours interval

Temperature upshift from 16 to 25 °C
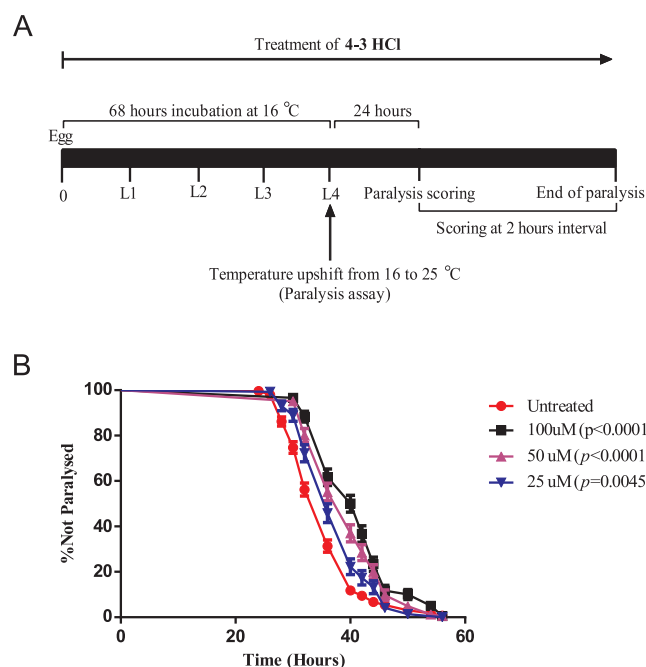(Paralysis assay)

B

Fig. 3. (A) Aβ-induced paralysis assay protocol. (B) Effect of **4-3 HCl** on the Aβ-induced paralysis in GMC101 nematodes. Time refers to hours after temperature up-shift. Incorporation of **4-3 HCl** into the agar media delayed the onset of paralysis, also suppressed the Aβ-induced paralysis (untreated *vs.* 100 μM, $p < 0.0001$; untreated *vs.* 50 μM, $p < 0.0001$; untreated *vs.* 25 μM, $p < 0.01$). Data are expressed as percentage of non-paralysed worms from at least three independent assays of > 100 worms in each experiment. The plot shown is representative of three experiments. Error bars = SEM.

3.3. Protective effect of 4-3 HCl against Aβ-induced paralysis in C. elegans

To determine whether **4-3 HCl** specifically protects against Aβ-induced toxicity, the Aβ-induced paralysis assay was performed using the transgenic *C. elegans* GMC101 that exhibits paralysis upon expression of human Aβ$_{1-42}$ in its bodywall muscle cells [24]. The transgenic GMC101 worms, after egg-synchronization, were incubated for 68 h at 16 °C on NGM plates pre-seeded with OP50. Paralysis of the worms was then induced by the transgene expression of human Aβ$_{1-42}$ in the muscle cells of the body wall triggered by a temperature up-shift from 16 °C to 25 °C. The treatment protocol (Fig. 3A) was such: the worms were fed with **4-3 HCl** (25, 50 and 100 μM) incorporated into the NGM agar, from the egg stage until the end of the paralysis assay. Untreated controls containing only NGM agar were used to monitor the normal rate of paralysis in the worm upon the temperature up-shift trigger. The paralysis of the worms was scored starting at 24 h after temperature up-shift. Compounds that possess neuroprotective effect against the Aβ toxicity in the transgenic worm will be able to increase the percentage of surviving worms and reduce the rate of Aβ-induced paralysis.

Fig. 3B shows the survival curves of the transgenic worms in the paralysis assay for the untreated control and **4-3 HCl** at 25 μM, 50 μM, and 100 μM from the start of temperature up-shift till the end of the assay. Treatment at different doses of **4-3 HCl** (25 μM, 50 μM, 100 μM) in the assay was observed to significantly increased the percentage of surviving worms over time as compared to the untreated control (untreated *vs.* 100 μM, $p < 0.0001$; untreated *vs.* 50 μM, $p < 0.0001$; untreated *vs.* 25 μM, $p < 0.01$), indicating that **4-3 HCl** offered some degrees of protection to the nematodes from paralysis induced by the Aβ expression in a concentration-dependent manner. In addition, the ability to delay the paralysis process was measured by determining the mean duration at which 50% of the worms were paralysed (PT$_{50}$) (Table 4). Treatment with **4-3 HCl** was shown to increase the PT$_{50}$ of Aβ-induced paralysis; however, it was only statistically significant at

Table 4
Mean durations at which 50% worms were paralysed (PT$_{50}$).* indicates significant difference *versus* untreated control at *p* value < 0.05.

Treatment	PT$_{50}$
Untreated Control	8.7 ± 0.6
4-3 HCl 100 μM	12.1 ± 0.6*
4-3 HCl 50 μM	9.9 ± 0.9
4-3 HCl 25 μM	10.3 ± 0.4

100 μM (untreated *vs* 100 μM, $p < 0.05$).

Interest in disorders involving amyloid misfolding and aggregation has increased over the past few years as studies have implicated these insoluble aggregates in the pathology of several neurodegenerative diseases including AD [31,32]. These toxic amyloid aggregates typically disrupt the internal and external cellular mechanisms leading to neuronal cell death; for this reason, efforts were made to find a reasonably useful model to unveil the mechanism underlying the aggregate toxicity and identify a neuroprotective strategy. In this respect, the *C. elegans* model has emerged as a useful tool to study the mechanism of Aβ toxicity. This model was able to identify compounds that demonstrated inhibitory activity on Aβ aggregation including the *Gingko biloba* extract EGb 761 [33], glycitein from soybeans [34] and reserpine [35], further supporting the model to associate Aβ inhibition to their protective activity against Aβ toxicity. In the present study, results showing the protective effect of **4-3 HCl** against the Aβ-induced paralysis indicated that this compound could attenuate the toxicity of Aβ expressed in the transgenic worm, which at least in part, may be attributed to its Aβ-aggregation inhibitory action shown in the *in vitro* assay. However, presently, the detailed mechanism was not further investigated. Nevertheless, the protective effect exhibited by **4-3 HCl** against the Aβ-induced paralysis would serve to motivate future investigation of the compound in a mammalian neurodegenerative model.

3.4. Protective effect conferred by 4-3 HCl on the 6-OHDA-induced dopaminergic neurodegeneration in C. elegans

The neuroprotective effect of **4-3 HCl** in *C. elegans* was further evaluated in the 6-OHDA-induced neurodegeneration model using the transgenic strain UA57 that expresses GFP in the dopaminergic (DAergic) neurons following the method described by Maranova and Nichols [25]. The treatment protocol was as follows: the egg-synchronized population of the transgenic worm was raised in the presence of various concentration of **4-3 HCl.** When the worms reached the L1 stage, they were incubated with 6-OHDA to induce degeneration of the DAergic neurons. Immediately after the 6-OHDA treatment, the worms were transferred to fresh NGM plate (with or without **4-3 HCl**). At 72 h post-6-OHDA exposure, the neuronal death of the DAergic neurons was determined by any diminishment or absence of the GFP-labelled DAergic neurons (Fig. 4).

The selected concentrations of **4-3 HCl** (25, 50 and 100 μM) used in the assay were initially checked for any detrimental effects that these concentrations may have on the DAergic neurons. In this preliminary test, the transgenic worms were incubated on the NGM plate supplemented with **4-3 HCl** at various concentrations (25, 50 and 100 μM) without exposing the L1 stage worms to 6-OHDA (the neurotoxin). These concentrations were found to be non-toxic to the nematodes (Fig. 5) and were thus used for the assay.

To assay the neuroprotective efficacy of **4-3 HCl**, the DAergic neuronal viability was evaluated by observing the loss of GFP reporter expression in the DAergic neurons of 6-OHDA-treated worms. Upon treatment with 6-OHDA, the cephalic (CEP) and anterior deirid (ADE) neurons of the transgenic worms exhibited a partial GFP loss or were altogether absent. When the 6-OHDA worms were treated with **4-3 HCl**, a noteworthy protection was observed in the DAergic neurons with CEP
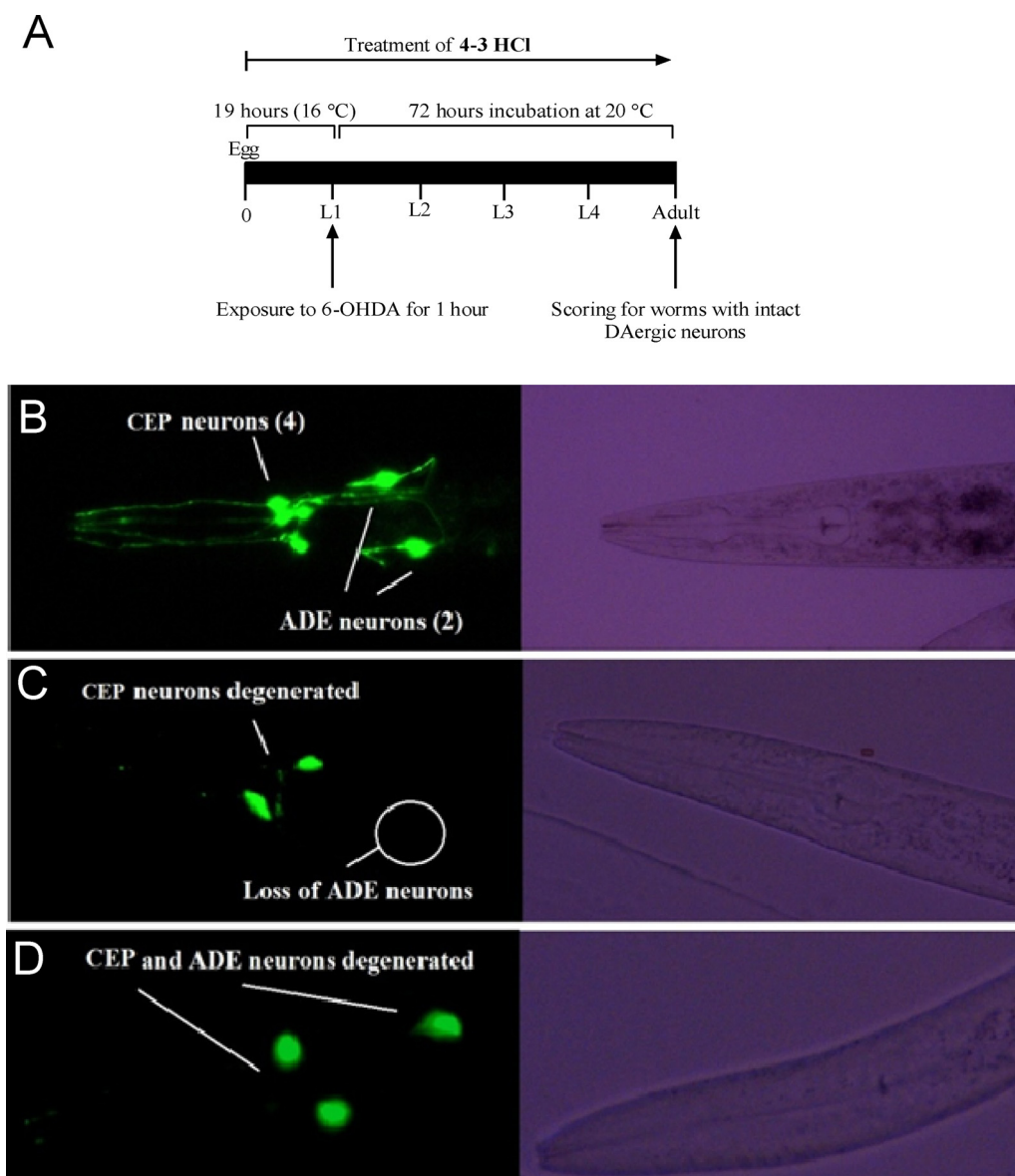
Fig. 4. (A) 6-OHDA-induced DAergic neurodegeneration assay protocol. Representative images of the head region with GFP expression pattern of DAergic neurons of *C. elegans* strain UA57, (B) worms with fully intact DAergic neurons, and (C–D) worms with patterns of DAergic neurons lost or degenerated. CEP = Cephalic neurons and ADE = Anterior deirid neurons. The left side shows the fluorescence images. The right side shows the differential interference contrast (DIC) images.

and ADE neurons retaining their GFP expression. Through examination of the GFP expression in the CEP and ADE neurons in each worm, the percentage of worms with intact DAergic neurons (no partial or complete loss) were scored for each group. At 72 h post-exposure to 5 mM of 6-OHDA for 1 h at the L1 stage, worms with fully intact DAergic neurons in the 6-OHDA-treated control were significantly reduced to approximately 16% ($p < 0.0001$) as compared to the normal control group (without any treatment) (Fig. 6). Treatment of **4-3 HCl** on the 6-OHDA-treated worms raised the percentage of worms with intact DAergic neurons in a dose-dependent manner. At 25 μM of **4-3 HCl**, the percentage of worms with intact DAergic neurons of the 6-OHDA worms increased by about 1.7 fold ($p < 0.05$), whereas worms exposed to 50 μM and 100 μM of **4-3 HCl** significantly increased the percentage of worm with intact DAergic neurons by 2.3 and 2.4 folds ($p < 0.0001$) respectively, as compared to the 6-OHDA-treated control, indicating that **4-3 HCl** was able to alleviate the DAergic degeneration induced by 6-OHDA.

Many studies reported that neuronal death or neurodegeneration induced by the neurotoxins such as 6-OHDA or 1-methyl-4-phenyl-1,2,3,6-tetrahydropyridine (MPTP) are associated with an increase in reactive oxygen species formation and toxin-induced mitochondrial dysfunction [36–38]. The molecular pathway through which these neurons degenerate is particularly dependent on the condition and neurotoxin used. In *C. elegans*, the administration of 6-OHDA produced a selective degeneration of the DAergic neurons, with dopamine transporter DAT-1 found to be mainly responsible for the uptake of 6-OHDA into the DAergic neurons [39]. The inhibition of DAT-1 activity was found to be able to prevent the damage to the neurons caused by 6-OHDA in *C. elegans* [25,40]. Thus, the neuroprotective activity against the 6-OHDA induced DAergic neurodegeneration displayed by **4-3 HCl** could be due to the inhibition of DAT-1 in the worm. However, further studies on this model when evaluating potential therapeutic compounds with various mechanisms of action besides DAT-1 inhibition [25,41] indicated that the protective effect of these various classes of drugs, some of them not DAT inhibitors, may not necessarily be due to DAT-1 inhibition. Other yet identified mechanisms may have contributed to the neuroprotection shown in this 6-OHDA-induced neurodegeneration model. Further investigation would be required to elucidate the
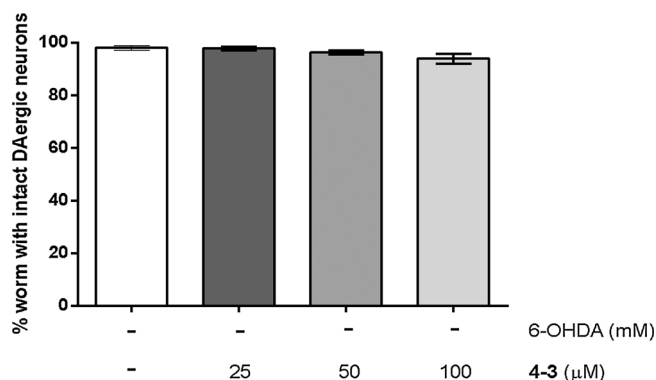
Fig. 5. Quantification of worms with intact DAergic neurons (without neurotoxin exposure). The transgenic strain UA57, raised in the presence or absence of **4-3 HCl** (25, 50 and 100 μM) on NGM plates from synchronized eggs to L1 stage for 19 h and further incubated for 72 h without the exposure to 6-OHDA. Data were presented as the mean percentage of worms with intact DAergic neurons from at least three independent assays of > 100 worms in each experiment. Error bars = SEM.

Fig. 6. Quantification of worms with intact DAergic neurons. The L1 worms of the transgenic strain UA57, raised in the presence or absence of **4-3 HCl** (25, 50 and 100 μM) from synchronized eggs, were exposed to the 6-OHDA and further incubated for 72 h in the presence or absence of **4-3 HCl** (25, 50 and 100 μM). Data were presented as the mean percentage of worms with intact DAergic neurons from at least three independent assays of > 100 worms in ea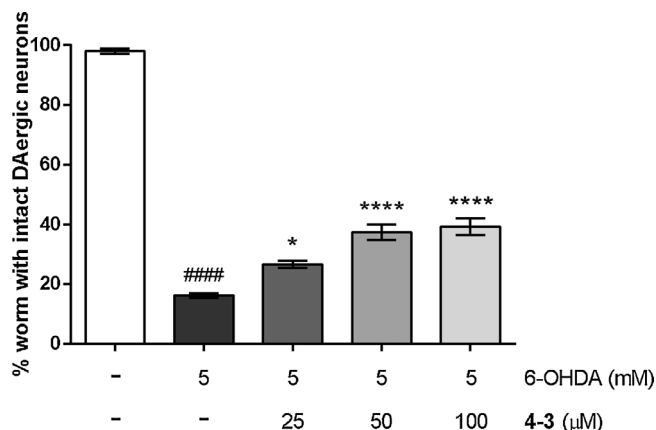ch experiment. Error bars = SEM. A hash (#) indicates significant differences between 6-OHDA-treated and untreated animals (#### $p < 0.0001$); an asterisk (*) indicates significant differences between the 6-OHDA-treated control and **4-3 HCl** + 6-OHDA-treated samples (*$p < 0.05$, ****$p < 0.0001$).

mechanism(s) underpinning **4-3 HCl** neuroprotective effect. Nevertheless, examination of the neuroprotective effect of **4-3 HCl** in this model has uncovered an additional neuroprotective aspect of the compound, which may be attributed to its multi-targeting potential.

4. Conclusion

The present investigation sought to explore the multi-targeting potential of amine- and carbamate-bearing aurones in two AD-related activities: MAO and Aβ aggregation inhibition. We have shown these two potentially neuroprotective modes of action in some of the aurones in addition to their previously reported anticholinesterase activity. With regards to the MAO inhibition, the aurones exhibited selective inhibition towards MAO-B. The better MAO-B inhibitors in this study were those with 6-methoxyl group attached at ring A. Among the different amine moieties attached as side chains, the most favoured was a pyrrolidine represented by aurone **2-2**. In the case of Aβ anti-aggregation activity, the most potent inhibitor identified was **4-3** (3′,4′,5′-

trimethoxyaurone) with a piperidine side chain at 6-position of ring A. **4-3** was observed to inhibit Aβ aggregation to a comparable extent as that of curcumin. In summary, a multi-targeting potential was uncovered in two anticholinesterase aurones: **2-2** with good MAO-B inhibition activity, and **4-3** which could inhibit Aβ. Further evaluation of the neuroprotective effect of the most promising aurone (**4-3**) with multi-targeting and optimum drug-like properties using two *C. elegans* neurodegeneration models, the Aβ-induced toxicity paralysis model and 6−OHDA-induced DAergic neurodegeneration model provides encouraging indications of neuroprotection in **4-3**. Evaluation on the Aβ-induced toxicity paralysis assay showed that **4-3 HCl** significantly delayed the paralysis of the transgenic worms in a dose dependent manner. Similarly, **4-3 HCl** significantly increased the percentage of worms with intact DAergic neurons in OHDA-treated nematodes. In conclusion, the results of this study indicated that aurone **4-3** has a general, non-specific neuroprotective property, as evidenced by the protection shown against two different neurotoxins (Aβ and 6-OHDA), which may be a translation of its multi-targeting property. The overall findings of the present study support the feasibility of the aurone scaffold for developing novel multi-targeting ligands as neuroprotective agents with favourable drug-like properties. Although the structural requirements for good activity in each AD-related activity (cholinesterase, MAO, and Aβ inhibition) were different among the aurones, at least one compound (**4-3**) in the present study stood out as having the best potential for further optimization. **4-3** represented a lead for the further refinement of the scaffold to give rise to a multi-targeting compound with optimal drug-like properties, worthy for the development into a novel therapeutic for neurodegenerative diseases including AD.

Declaration of interest

The authors declare that there is no conflict of interest.

Acknowledgements

Appendix A. Supplementary data

Supplementary material related to this article can be found, in the online version, at doi:https://doi.org/10.1016/j.biopha.2018.11.054.

References

[1] R. Leon, A.G. Garcia, J. Marco-Contelles, Recent advances in the multitarget-directed ligands approach for the treatment of Alzheimer's disease, Med. Res. Rev. 33 (2013) 139–189.

[2] R.T. Bartus, R.L. Dean, B. Beer, A.S. Lippa, The cholinergic hypothesis of geriatric memory dysfunction, Science 217 (1982) 408–414.

[3] J. Hardy, D. Allsop, Amyloid deposition as the central event in the aetiology of Alzheimer's disease, Trends Pharmacol. Sci. 12 (1991) 383–388.

[4] V. Garcia-Escudero, P. Martin-Maestro, G. Perry, J. Avila, Deconstructing mitochondrial dysfunction in Alzheimer disease, Oxid. Med. Cell. Longev. 12 (2013) 1–13.

[5] L. Trillo, D. Das, W. Hsieh, B. Medina, S. Moghadam, B. Lin, V. Dang, M.M. Sanchez, Z. De Miguel, J.W. Ashford, A. Salehi, Ascending monoaminergic systems alterations in Alzheimer's disease, translating basic science into clinical care, Neurosci. Biobehav. Rev. 37 (2013) 1363–1379.

[6] H.W. Klafki, M. Staufenbiel, J. Kornhuber, J. Wiltfang, Therapeutic approaches to Alzheimer's disease, Brain 129 (2006) 2840–2855.

[7] W.L. Klein, Synaptotoxic amyloid-β oligomers: a molecular basis for the cause, diagnosis, and treatment of Alzheimer's disease? J. Alzheimers Dis 33 (2013) 49–65.

[8] I. Benilova, E. Karran, B. De Strooper, The toxic Aβ oligomer and Alzheimer's disease: an emperor in need of new clothes, Nat. Neurosci. 15 (2012) 349–357.

[9] K.J. Reinikainen, L. Paljarvi, T. Halonen, O. Malminen, V.M. Kosma, M. Laakso, P.J. Riekkinen, Dopaminergic system and monoamine oxidase B activity in

Alzheimer's disease, Neurobiol. Aging 9 (1988) 245–252.

[10] M.E. Gotz, P. Fischer, W. Gsell, P. Riederer, M. Streifler, M. Simanyi, F. Muller, W. Danielczyk, Platelet monoamine oxidase B activity in dementia: a 4-year follow-up, Dement. Geriatr. Cogn. Disord. 9 (1998) 74–77.

[11] B. Gulyas, E. Pavlova, P. Kasa, K. Gulya, L. Bakota, S. Varszegi, E. Keller, M.C. Horvath, S. Nag, I. Hermecz, K. Magyar, C. Halldin, Activated MAO-B in the brain of alzheimer patients, demonstrated by [^{11}C]-*L*-deprenyl using whole hemisphere autoradiography, Neurochem. Int. 58 (2011) 60–68.

[12] S. Jo, O. Yarishkin, Y.J. Hwang, Y.E. Chun, M. Park, D.H. Woo, J.Y. Bae, T. Kim, J. Lee, H. Chun, H.J. Park, D.Y. Lee, J. Hong, H.Y. Kim, S.J. Oh, S.J. Park, H. Lee, B.E. Yoon, Y.S. Kim, Y. Jeong, I. Shim, Y.C. Bae, J. Cho, N.W. Kowall, H. Ryu, E. Hwang, D. Kim, C.J. Lee, GABA from reactive astrocytes impairs memory in mouse models of Alzheimer's disease, Nat. Med. 20 (2014) 886–896.

[13] O. Weinreb, T. Amit, O. Bar-Am, M.B. Youdim, Ladostigil: a novel multimodal neuroprotective drug with cholinesterase and brain-selective monoamine oxidase inhibitory activities for Alzheimer's disease treatment, Curr. Drug. Targets 13 (2012) 483–494.

[14] E. Borroni, R. Wyler, J. Messer, S. Nave, A. Desura, Preclinical characterization of RO4602522, a novel, selective and orally active monoamine oxidase type B inhibitor for the treatment of Alzheimer's disease, Alzheimers Dement. 9 (2013) 818.

[15] E. Nepovimova, E. Uliassi, J. Korabecny, L.E. Peña-Altamira, S. Samez, A. Pesaresi, G.E. Garcia, M. Bartolini, V. Andrisano, C. Bergamini, R. Fato, D. Lamba, M. Roberti, K. Kuca, B. Monti, M.L. Bolognesi, Multitarget drug design strategy: quinone–tacrine hybrids designed to block amyloid-β aggregation and to exert anticholinesterase and antioxidant effects, J. Med. Chem. 57 (2014) 8576–8589.

[16] M. Rosini, V. Andrisano, M. Bartolini, M.L. Bolognesi, P. Hrelia, A. Minarini, A. Tarozzi, C. Melchiorre, Rational approach to discover multipotent anti-alzheimer drugs, J. Med. Chem. 48 (2005) 360–363.

[17] H.Y. Zhang, One-compound-multiple-targets strategy to combat Alzheimer's disease, FEBS Lett. 579 (2005) 5260–5264.

[18] K.F. Liew, K.L. Chan, C.Y. Lee, Blood-brain barrier permeable anticholinesterase aurones: synthesis, structure-activity relationship, and drug-like properties, Euro J. Med. Chem. 94 (2015) 195–210.

[19] K.F. Liew, N.A. Hanapiah, K.L. Chan, S.R. Yusof, C.Y. Lee, Assessment of the blood-brain barrier permeability of potential neuroprotective aurones in parallel artificial membrane permeability assay and porcine brain endothelial cell models, J. Pharm. Sci. 106 (2017) 502–510.

[20] W.J. Geldenhuys, M.O. Funk, C.V. Schyf, R.T. Carroll, A scaffold hopping approach to identify novel monoamine oxidase B inhibitors, Bioorg. Med. Chem. Lett. 22 (2012) 1380–1383.

[21] N. Morales-Camilo, C.O. Salas, C. Sanhueza, C. Espinosa-Bustos, S. Sepúlveda-Boza, M. Reyes-Parada, F. Gonzalez-Nilo, M. Caroli-Rezende, A. Fierro, Synthesis, biological evaluation, and molecular simulation of chalcones and aurones as selective MAO-B inhibitors, Chem. Biol. Drug. Des. 85 (2015) 685–695.

[22] Y. Maya, M. Ono, H. Watanabe, M. Haratake, H. Saiji, M. Nakayama, Novel radioiodinated aurones as probes for SPECT imaging of beta-amyloid plaques in the brain, Bioconjug. Chem. 20 (2009) 95–101.

[23] A. Holt, D.F. Sharman, G.B. Baker, M.M. Palcic, A continuous spectrophotometric assay for monoamine oxidase and related enzymes in tissue homogenates, Anal. Biochem. 244 (1997) 384–392.

[24] V. Dostal, C.D. Link, Assaying β-amyloid toxicity using a transgenic *C. elegans* model, J. Vis. Exp. 44 (2010) 1–4.

[25] M. Marvanova, C.D. Nichols, Identification of neuroprotective compounds of

[26] C. Lu, Q. Zhou, J. Yan, Z. Du, L. Huang, X. Li, A novel series of tacrineselegiline hybrids with cholinesterase and monoamine oxidase inhibition activities for the treatment of Alzheimer's disease, Eur. J. Med. Chem. 62 (2013) 745–753.

[27] Y. Sun, J. Chen, X. Chen, L. Huang, X. Li, Inhibition of cholinesterase and monoamine oxidase-B activity by tacrine-homoisoflavonoid hybrids, Bioorg. Med. Chem. 21 (2013) 7406–7417.

[28] R.S. Li, X.B. Wang, X.J. Hu, L.Y. Kong, Design, synthesis and evaluation of flavonoid derivatives as potential multifunctional acetylcholinesterase inhibitors against Alzheimer's diseases, Bioorg. Med. Chem. Lett. 23 (2013) 2636–2641.

[29] H. Frankowski, S. Alavez, P. Spilman, K.A. Mark, J.D. Nelson, P. Mollahan, R.V. Rao, S.F. Chen, G.J. Lithgow, H.M. Ellerby, Dimethyl sulfoxide and dimethyl formamide increase lifespan of *C. elegans* in liquid, Mech. Ageing Dev. 134 (2013) 69–78.

[30] X. Wang, X. Wang, L. Li, D. Wang, Lifespan extension in *Caenorhabditis elegans* by DMSO is dependent on sir-2.1 and daf-16, Biochem. Biophys. Res. Commun. 400 (2010) 613–618.

[31] J. Hardy, D.J. Selkoe, The amyloid hypothesis of Alzheimer's disease: progress and problems on the road to therapeutics, Science 297 (2002) 353–356.

[32] R.E. Tanzi, L. Bertram, Twenty years of the Alzheimer's disease amyloid hypothesis: a genetic perspective, Cell 120 (2005) 545–555.

[33] Y. Wu, Z. Wu, P. Butko, Y. Christen, M.P. Lambert, W.L. Klein, C.D. Link, Y. Luo, Amyloid-beta-induced pathological behaviors are suppressed by *Ginkgo biloba* extract EGb 761 and ginkgolides in transgenic *Caenorhabditis elegans*, J. Neurosci. 26 (2006) 13102–13113.

[34] A. Gutierrez-Zepeda, R. Santell, Z. Wu, M. Brown, Y. Wu, I. Khan, C.D. Link, B. Zhao, Y. Luo, Soy isoflavone glycitein protects against beta amyloid-induced toxicity and oxidative stress in transgenic Caenorhabditis elegans, BMC Neurosci. 6 (2005) 1–9.

[35] U. Arya, H. Dwivedi, J.R. Subramaniam, Reserpine ameliorates Abeta toxicity in the Alzheimer's disease model in Caenorhabditis elegans, Exp. Gerontol. 44 (2009) 462–466.

[36] R. Nass, D.H. Hall, D.M. Miller III, R.D. Blakely, Neurotoxin-induced degeneration of dopamine neurons in *Caenorhabditis elegans*, Proc. Natl. Acad. Sci. U. S. A. 99 (2002) 3264–3269.

[37] Y. Glinka, M. Gassen, M.B. Youdim, Mechanism of 6-hydroxydopamine neurotoxicity, J. Neural Transm. Suppl. 50 (1997) 55–66.

[38] J.A. Javitch, R.J. D'Amato, S.M. Strittmatter, S.H. Snyder, Parkinsonism-inducing neurotoxin, *N*-methyl-4-phenyl-1,2,3,6-tetrahydropyridine: uptake of the metabolite *N*-methyl-4-phenylpyridine by dopamine neurons explains selective toxicity, Proc. Natl. Acad. Sci. U. S. A. 82 (1985) 2173–2177.

[39] C. Sachs, G. Jonsson, Mechanisms of action of 6-hydroxydopamine, Biochem. Pharmacol 24 (1975) 1–8.

[40] R. Nass, M.K. Hahn, T. Jessen, P.W. McDonald, L. Carvelli, R.D. Blakely, A genetic screen in Caenorhabditis elegans for dopamine neuron insensitivity to 6-hydroxydopamine identifies dopamine transporter mutants impacting transporter biosynthesis and trafficking, J. Neurochem. 94 (2005) 774–785.

[41] R.H. Fu, Y.C. Wang, C.S. Chen, R.T. Tsai, S.P. Liu, W.L. Chang, H.L. Lin, C.H. Lu, J.R. Wei, Z.W. Wang, W.C. Shyu, S.Z. Lin, Acetylcorynoline attenuates dopaminergic neuron degeneration and α-synuclein aggregation in animal models of Parkinson's disease, Neuropharmacology 82 (2013) 108–120.

Caenorhabditis elegans dopaminergic neurons against 6-OHDA, J. Mol. Neurosci. 31 (2007) 127–137.